Planning for Distribution Resilience under Variable Generation: Prevention, Surviving and Recovery

Tongdan Jin¹, Nhi Mai¹, Yi Ding², Long Vo¹, Rana Dawud¹

¹ Ingram School of Engineering
Texas State University, San Marco, TX 7866, USA
{tj17@, nm1178@, lv1098@, rd1156@txstate.edu}

² School of Electrical Engineering
Zhejiang University, Hangzhou, Zhejiang, 310000, China
{yiding@zju.edu.cn}

Abstract—Power grids based on traditional N-1 design criteria are no longer adequate because these designs do not withstand extreme weather events or cascading failures. Microgrid system has the capability of enhancing grid resilience through defensive or islanded operations in contingency. This paper presents a probabilistic framework for planning resilient distribution system via distributed wind and solar integration. We first define three aspects of resilient distribution system, namely prevention, survivability and recovery. Then we review the distributed generation planning models that comprehend moment estimation, chance constraints and bi-directional power flow. We strive to achieve two objectives: 1) enhancing the grid survivability when distribution lines are damaged or disconnected in the aftermath of disaster attack; and 2) accelerating the recovery of damaged assets through pro-active maintenance and repair services. A simple 9-node network is provided to demonstrate the application of the proposed resilience planning framework.

Keywords—microgrid; extreme weather; resilience; distributed generation; central limit theorem

I. Nomenclature

Y, y= Random wind speed, and its realization

 $f_w(y)$ = Wind speed probability density function

 $F_{w}(y)$ = Wind speed cumulative distribution function

c, d= Weibull scale and shape parameters for Y

 P_m = Rated power for wind turbine

 $P_{w}(Y)$ = Wind turbine output power at wind speed Y

 v_c , v_r , v_s = Cut-in, rated, and cut-off speeds, respectively

 η_{max} = Conversion rate from wind to electric power

 ρ = Air density

A= Area covered by wind turbine blades

 $\gamma = 0.5 \eta_{\text{max}} \rho A$

m= Number of DER types in the DG system

n= Number of nodes in the DG system

l= Number of branches in the DG system

 $P_s(S)$ = PV output power

S, s= Solar irradiance and its realization,

respectively

 $f_s(s)$ = Beta distribution function for solar irradiance

a, b= Beta distribution parameter

 s_m = Maximum solar irradiance (W/m^2)

 η_s = Photovoltaic conversion efficiency

 A_s = PV panel area (m^2)

 T_o = PV operating temperature (°C)

 P_{ii}^{c} Power capacity of DER type i at node j

 P_{ij} = Instant output power of DER type *i* at node *j*,

a random variable

D= Total system demand, a random variable

 D_i = Demand at node j, a random variable

 $R_i(t)$ = Reliability function for DER type i

 η_i , β_i = Scale and shape parameters in $R_i(t)$

 $u(\tau)$ = DER maintenance cost per unit time

 $c^{(f)}$ = Cost for performing a corrective maintenance

 $c^{(p)}$ = Cost for performing a planned maintenance

 t_f , t_p = Failure and planned downtimes, respectively

 t_a = Annual operating hours for DER units

 $A(\tau)$ = Availability of a single DER unit

 $A_{DG}(\tau)$ = Availability of the DG system group

K= Number of branches prone to failure in extreme weather

R= Number of repair teams

 λ = Failure rate of branches in extreme weather

 μ = Repair rate of branches in extreme weather

T= Number of planning years

 C_{DG} = Annualized DG system cost

 $\phi(r, h)$ = Formula for computing present annuity

r= Annual compound interest rate

h= Years for paying off the DER capital

 a_{ij} = Cost per MW of installing DER type i at node j

 b_{ij} Operation cost per MWh for DER i at node j

Credits or penalty per MWh for putting DER *i* at node *j*

 V_{DG} = Nominal voltage of the DG system

 $\mu_{V_{u}(\mathbf{x})}$ = Mean voltage at node j in year t

 σ_{v_i} = Voltage standard deviation at node *j* in year *t*

 V_{\min} = Low voltage limit

 V_{max} = Upper voltage limit

 α_{l} = Loss-of-load probability criterion

 $\alpha =$ Confidence level for voltage variation

 x_{ij} DER type *i* at node *j* in year *t*, binary decision

 z_{ijt} = Cumulative number of DER type i at node j by year t, and $z_{iit} = \sum_{k=1}^{t} x_{iit}$

 t_i = Maintenance time of DER i, decision variable

II. INTRODUCTION

Electric distribution grid planning has long focused on the reliability, affordability, and efficiency of power delivery to end users; however, this focus has primarily been outside the realm of natural disasters. Enhancing the resilience of electric



grid against extreme weather events becomes a fundamental task for all the stakeholders in generation, transmission and distribution sectors. According to [1], resilience is defined as the ability of a power system to anticipate, resist, absorb, respond to, adapt to, and recover from unexpected disruptions. Panteli and Mancarella [2] state that events considered in resilience management differs from reliability analysis owing to two unique features: 1) high impact with low probability of occurrence; and 2) catastrophic consequence resulted from cascading failures.

Natural disasters like earthquakes, tsunami, hurricanes, and tornados have caused tremendous economic losses. environmental damages and human casualties, rendering the traditional N-1 reliability criterion ineffective to withstand these extreme events. For instance, Hurricane Sandy was an N-90 event with estimated economic losses up to \$50 billion. As a result, power outages throughout the eastern US lasted up to 30 days [3]. Extreme events are also responsible for the common cause failures that occur when two or more infrastructures are affected simultaneously. In fact, most cascading failures in power system occur largely due to the common cause failures. Zhou et al. [4] investigate the 2008 Great Ice Storm in Southern China, and find that interdependency of coal mining, supply lifeline, and harsh weather created cascading effects on the electric power supply network. This led to a series of failures in regional power generation and delivery processes, causing the loss of power to nearly 15 million homes in Southern China.

Distributed generation (DG) system integrating wind and solar power is emerging as a new energy supply method to meet the growing electricity demand and environmental requirements. Unlike a central power plant, the capacity of distributed energy resource (DER) is relatively small and less than 10 MW, while the capacity of a central generating unit often exceeds 500 MW. Typical DER units include wind turbines (WT), solar photovoltaic (PV), fuel cells, diesel generators, micro-turbines, combined heat and power, and small-size batteries. They can be installed in the distribution network or at the consumption sites. WT and PV are in particular appealing because of their zero emissions and no use of fossil fuels.

In addition to environmental sustainability, DG technology fosters the energy independence, saves the transmission expansion cost, and improves grid resilience in extreme events. A good example of resilience performance is the Roppongi Hills microgrid in Tokyo. During the Great East Japan earthquake in 2011, natural gas based Roppongi Hill microgrids was able to maintain electricity supply even though the main grid was dysfunctional for several days, highlighting the grid survivability via microgrid operation in adverse condition [5]. The world-wide installation of DER units and microgrid capacity consistently increases in the last decade. In 2012 alone the new installation of DER reached 142 GW, representing 39% share of the new capacity addition of that year [6]. The rise of DG systems opens the way for designing and operating resilient distribution grid via microgrid integration.

This paper presents a probabilistic framework for designing resilient distribution system through the integration of onsite wind and solar generation. We aim to achieve two objectives: 1) enhancing the grid survivability when the distribution lines are damaged or disconnected post the

disaster attack; and 2) accelerating the restoration of damaged utility assets through pro-active maintenance and repair services. To these ends, we first define three resilience aspects pertaining to distribution systems. Then, we review the moment-based modeling approach to analyzing the power intermittency, voltage variation and bidirectional power flow.

The remainder of the paper is organized as follows. Section 3 elaborates three key aspects of distribution resilience. Section 4 characterizes the intermittency of wind and solar generation and their impacts on power quality. Sections 5 discusses the prevention and recovery aspects via pro-active maintenance and repair policy. Section 6 formulates a simple DG planning model to enhance the grid survivability through defensive microgrid operation. In Section 7, we demonstrate the proposed planning model on a 9-node distribution network. Section 8 concludes the paper.

III. THREE ASPECTS OF DISTRIBUTION RESILIENCE

A. Literature Review

Significant research effort has been focused on optimal design of the distribution grid, with many approaches incorporating integrated resilience features. We briefly survey the literature in this area.

Hardening is an effective approach to attaining the grid resilience by adding redundant lines, using underground cables, fortifying poles, elevating substation, and trimming vegetation [7], [8]. Recently, the development of aerial drone programs to assess storm damage and tree vegetation can provide onsite real-time data of electricity infrastructure. In general, upgrading power infrastructure could be costly in terms of materials, labor and time. It could also be constrained by environmental policies and government regulation.

An alternative approach to power resilience is to develop active distribution networks in which DER units or microgrid systems serve as backup units or operate in islanded mode in contingency. Kwasinski et al. [9] assess the availability of different DER units upon natural disaster onslaught, and find that WT and PV outperform fuel-based generators because the fossil fuel supply line could be damaged post the disaster attack. Liu et al. [10] use Monte Carlo simulation to compare the resilience between network hardening, topology reconfiguration and microgrid operations on IEEE 30-bus and 118-bus systems. Shao [11] propose a cogeneration model to enhance the energy resilience using distribution electricity and natural gas system. Panteli et al. [12] propose a set of severity risk index to determine the creation of defensive island microgrid when current network topology and the branches are at higher risk of tripping due to severe weather. Bie et al. [13] present a quantitative framework to evaluate power grid resilience using metrics like LOLP and EDNS. These studies agree that topology reconfiguration and defensive microgrid are effective to strengthen the distribution resilience.

B. The Three Aspects of Distribution Resilience

According to EPRI [14], grid resiliency is manifested in three aspects: prevention, survivability, and recovery.

Prevention aims to protect the distribution system from being damaged by extreme weather, intentional attacks or other unexpected disasters. To that end, innovations are required to be developed and included in existing design standards, construction guidelines, and maintenance and inspection procedures.

Survivability refers to the ability to maintain the basic level of power supply to consumers in the event of a complete loss of electrical service post the disaster event. The key elements of survivability include the use of defensive microgrid systems and mobile generators to power critical infrastructures, including traffic signals, banks, hospitals, schools, and communication equipment.

Recovery means the resiliency planner ought to provide quick assessment on damaged grid, promptly deploy crew to damaged assets and timely replace and repair failed circuits or components. In recent storms such as Hurricane Harvey. accessing affected areas was problematic because it is difficult to route crews through streets that were blocked by fallen trees and flooded zones [15].

C. The Objective and Contribution of This Paper

Based on the three resilience aspects, this paper aims to propose a probabilistic framework to integrate these aspects into the planning and operation of active distribution grid. The contributions of this paper are summarized as follow: First, unlike most literature that address one aspect of distribution resilience, we propose a holistic resilience planning framework in which prevention, survivability and recovery are jointly taken into account. Second, we leverage machine-repairman model to address the recovery process of damaged lines, which is rarely reported in previous literature.

IV. MOMENTS OF WIND AND SOLAR POWER

In order to design a resilient and robust DG system, the intermittency of renewable generation shall be analyzed and appropriately incorporated into the planning model. We adopt the moment method to characterize the power intermittency of wind and solar units. A major advantage of the moment method is that an explicit distribution of the DER power is not required.

A. Modelling Wind Generation

In this section, we review the moment method for modelling variable generation which is originally from [16]. Let $P_{w}(y)$ be the instantaneous power at wind speed y, the following cubic power curve has been widely used to estimate the instantaneous WT power.

$$P_{w}(y) = \begin{cases} 0, & 0 < y < v_{c}, \ y > v_{s} \\ 0.5\eta_{\text{max}} \rho A y^{3}, & v_{c} \leq y \leq v_{r} \\ P_{m}, & v_{r} \leq y \leq v_{s} \end{cases}$$
(1)

The power curve is segmented by three characteristic wind speeds: v_c is the cut-in speed; v_r is the rated speed; and v_s is the cut-off speed. Note that P_m is the rated power. ρ is the air density, and A is the area covered by the blades of WT. η_{max} is the energy conversion rate. The theoretical value of η_{max} is 0.5926, but the actual value usually is lower and within [0.3, 0.5]. Without loss of generality, the Weibull distribution is used to characterize the annual wind speed profile. The Weibull probability density function $f_w(y)$ and the cumulative distribution functions $F_w(y)$ are

$$f_w(y) = \left(\frac{d}{c}\right) \left(\frac{y}{c}\right)^{d-1} e^{-(y/c)^d}, \qquad (2)$$

$$F_w(y) = 1 - e^{-(y/c)^d}$$
, (3)

where, c and d are the scale and shape parameters. Based on equations (1) and (2), the mean, the second moment, and the variance of the wind power are estimated by

$$E[P_{w}(Y)] = \int_{0}^{+\infty} P_{w}(y) f_{w}(y) dy$$

$$= \gamma \int_{v_{c}}^{v_{r}} x^{3} f_{w}(y) dx + P_{m}(F_{w}(v_{s}) - F_{w}(v_{r})), \qquad (4)$$

$$E[P_{w}^{2}(Y)] = \gamma^{2} \int_{v_{c}}^{v_{r}} x^{6} f_{w}(y) dx + P_{m}^{2}(F_{w}(v_{s}) - F_{w}(v_{r})), \qquad (5)$$

$$E[P_w^2(Y)] = \gamma^2 \int_{v_c}^{v_r} x^6 f_w(y) dx + P_m^2 (F_w(v_s) - F_w(v_r)), \quad (5)$$

$$var(P_{w}(Y)) = E[P_{w}^{2}(Y)] - (E[P_{w}(Y)])^{2},$$
 (6)

where $\gamma = 0.5 \eta_{\text{max}} \rho A$. In general the mean and the variance are sufficient to characterize the wind power intermittency. Although closed-form expressions are unavailable for equations (4) and (6), numerical methods can be easily used to compute $E[P_w(Y)]$ and $var(P_w(Y))$.

B. Modelling Solar PV Generation

The output power of a PV system depends on multiple factors, including the panel area, the conversion efficiency, the operating temperature, the panel orientation, the tilt angle, the calendar date, the daily hour, the latitude, and the weather condition [17]. A generic PV power model incorporating all these factors is given by

$$P_s(s) = \eta_s A_s s(1 - 0.005(T_o - 25)) = \delta s$$
, (7)

With
$$\delta = \eta_s A_s (1 - 0.005(T_o - 25))$$
. (8)

Here, $P_s(s)$ is the instantaneous PV power, η_s is the PV efficiency with $\eta_s=10-15\%$, A_s is the panel area. T_o is the PV operating temperature (${}^{\circ}C$), and s is the solar irradiance (in unit of W/m^2) incident on the panel surface. Let S be the random variable representing the solar irradiance, and s is its realization. Then, the beta distribution for S during the course of a year can be stated as follows [18].

$$f_s(s) = \frac{\Gamma(a+b)}{s_m \Gamma(a) \Gamma(b)} \left(\frac{s}{s_m}\right)^{a-1} \left(1 - \frac{s}{s_m}\right)^{b-1}, \text{ for } 0 \le s \le s_m \quad (9)$$

where, a and b are the shape parameters of the distribution. s_m is the maximum irradiance in a year. Based on equations (7) and (9), the mean, and the variance of $P_s(s)$ are obtained as

$$E[P_s(S)] = \int_0^{s_m} P_s(s) f_s(s) ds = \frac{a \delta s_m}{a+b} , \qquad (10)$$

$$var(P_s(S)) = \frac{ab\,\delta^2 s_m^2}{(a+b)^2 (a+b+1)} \,. \tag{11}$$

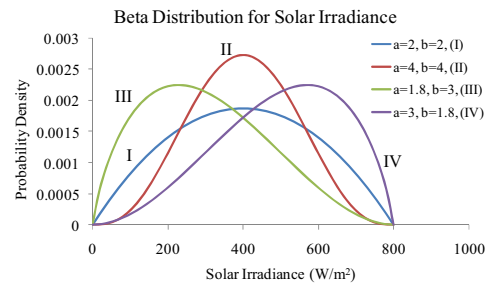


Fig. 1. Annual Solar Irradiance Distributions

Fig. 1 shows various types of beta probability density functions to mimic different solar irradiance profile during the course of a year. Note that all curves are plotted assuming s_m =800 W/m^2 .

C. Moments of System Power and Load

We define several notations before presenting the aggregate system power. Let m be the number of the DER types that are potentially placed in the distribution network. Let n be the number of nodes where DER units can be placed. Let x_{ij} be the integer denoting the number of units of DER type i to be placed at node j. Then $\mathbf{x} = [x_{11}, x_{12}, ..., x_{mn}]$ is the decision vector corresponding to the DER sizing and siting in the distribution network. Let $P(\mathbf{x})$ and D be the aggregate system power and load, respectively. Then,

$$P(\mathbf{x}) = \sum_{i=1}^{m} \sum_{j=1}^{n} x_{ij} P_{ij} , \qquad (12)$$

$$D = \sum_{j=1}^{n} D_{j}, \qquad (13)$$

where P_{ij} is a random variable representing the power output of a single unit of DER type i at node j. Note D_j is a also random variable representing the demand at node j. We can further estimate the mean and the variance of $P(\mathbf{x})$ and D as

$$\mu_{P(\mathbf{x})} = E[P(\mathbf{x})] = \sum_{i=1}^{m} \sum_{j=1}^{n} x_{ij} E[P_{ij}], \qquad (14)$$

$$\sigma_{P(\mathbf{x})}^2 = \text{var}(P(\mathbf{x})) = \sum_{i=1}^{m} \sum_{j=1}^{n} x_{ij}^2 \text{var}(P_{ij}),$$
 (15)

$$\mu_{D} = E[D] = \sum_{i=1}^{n} E[D_{i}],$$
 (16)

$$\sigma_D^2 = \operatorname{var}(D) = \sum_{j=1}^n \operatorname{var}(D_j). \tag{17}$$

D. Power Quality Criterion

In power industry, LOLP is a fundamental metric used to monitor and control the service reliability. It is defined as the probability that the power is less than the demand at any time. Then LOLP can be defined as

$$P\{P(\mathbf{x}) < D\} \le \alpha_1,\tag{18}$$

where α_1 is the probability of power outage that should be kept as small as possible.

The central limit theorem (CLT) states that the sum of the mutually independent random variables having limited mean and variance tends to be normally distributed. CLT is still valid when individual variables are weakly correlated. Based on CLT, it is safe to claim that D is normally distributed regardless the underlying distribution of D_j . Assuming nodal generation and loads are mutually independent, based on CLT Equation (18) can be translated into its deterministic counterpart as follows,

$$\mu_{P(\mathbf{x})} \ge \mu_D + Z_{1-\alpha_i} (\sigma_{P(\mathbf{x})}^2 + \sigma_D^2)^{1/2},$$
 (19)

where, $Z_{1-\alpha_i}$ is the Z-value of the standard normal distribution. The inequality shows that injecting DER units is able to increase the mean power, yet the overall variance also increases. Last but not the least, the moment method in Equations (14)-(17) actually relax the normality assumption that are often imposed on P_{ij} and D_i in existing literature.

V. PLANNING FOR PREVENTION AND RECOVERY

A. Prevention through Scheduled Maintenance

System availability can be improved through preventative maintenance (PM) by pro-actively inspecting and replacing aging pats prior to their failure. Age-based PM is perhaps the most widely used maintenance strategy in power industry because of its scheduling flexibility and easy management [19], [20]. When generating units are maintained under age-based PM policy, the goal is to find the optimum maintenance interval τ^* such that the maintenance cost per unit time, denoted as $u(\tau)$, is minimized. Such an optimum interval can be determined by minimizing the following equation [21].

$$\min_{\tau} u(\tau^*) = \frac{c^{(f)} F(\tau) + c^{(p)} R(\tau)}{\int_0^{\tau} R(z) dz},$$
(20)

where, $R(\tau)$ is the reliability function of a DER unit and $F(\tau)$ is the cumulative distribution function with $F(\tau)=1$ - $R(\tau)$. Parameters $c^{(f)}$ and $c^{(p)}$ represent the cost for performing a failure replacement and a planned replacement, respectively. Typically $c^{(f)} >> c^{(p)}$, because the downtime cost of an unexpected failure is much higher than a planned replacement.

Due to its versatile shapes, the Weibull distribution is perhaps the most widely used model to estimate the lifetime of systems. The Weibull reliability function is often expressed as

$$R(t) = \exp\left(-\left(\frac{t}{\eta}\right)^{\beta}\right)$$
, with $\eta, \beta > 0$ (21)

where η and β are the scale and shape parameters, respectively. By changing β (i.e. β <1, β =1, or β >1), equation (21) can characterize decreasing, constant, and increasing failure rates. Distinctions must be made between equation (2) and equation (21). In the former, the Weibull distribution is used to model the random behavior of wind speed. Here it is used to estimate the time-to-failure of DER units.

B. Operational Availability of DG System

High equipment availability is desirable to maximize the energy throughput given the intermittent wind speed and solar radiation. Equipment availability is usually defined as the ratio of the uptime over the sum of the uptime and downtime. Let A be the availability of a DER unit, then

$$A(\tau) = \frac{\int_0^{\tau} R(z)dz}{\int_0^{\tau} R(z)dz + t_p R(\tau) + t_f F(\tau)},$$
 (22)

where, t_p and t_f represent the downtime duration for a planned and a failure replacement, respectively. In general $t_p < t_f$, because in a planned maintenance, the spare parts and the labor can be prepared in advance, avoiding unnecessary delays otherwise occurring in an unexpected failure.

Before deriving the availability model for the entire DG system group, let i=1, 2, ..., m be the index denoting the available DER types including the substation. For instance, if the generator pool consist of 1 MW WT, 1.5 MW WT, and 0.5 MW PV, and 10 MW substation, then i=1, 2, 3, and 4. The availability of the entire DG group can be expressed as

$$A_{DG}(\tau) = \prod_{i=1}^{m} \prod_{j=1}^{n} (A_i(\tau_i))^{x_{ij}} . \tag{23}$$

Equation (23) is obtained assuming the reliability of the DG system group is equivalent to a series system. $A_i(\tau_i)$ is the availability of DER type i as defined in equation (22), and x_{ij}

is an integer variable representing whether DER type i is installed on node j or not. For instance, if x_{ij} =1, meaning one unit of DER type i is installed at node j, or x_{ij} =0 otherwise. In (23), it is also assumed that the DER units of the same type adopt the same maintenance schedule, regardless of their physical locations. This assumption, however, can be relaxed if τ_i is location-dependent in the distribution network.

C. Repair and Recovery Model

The recovery or restoration process of distribution branches can be treated as machine-repairman problem. Let K be the number of distribution branches that are susceptible to failure in the extreme weather. Let R be the available teams to repair and restore the damaged distribution branches. The transition diagram of the restoration process is given as follows,

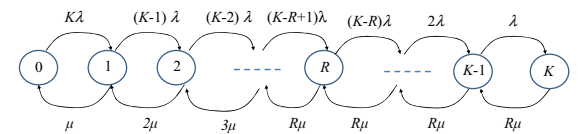


Figure 2. Transition Diagram of Repairing Distribution Lines

Note that the time-to-failure of distribution branches is assumed to be exponentially distributed with rate λ (i.e. failures per unit time) during the extreme weather period. Similarly the time-to-recovery of damaged branch is also exponential with the repair rate μ (i.e. number of lines repaired per unit time). Here failure means a line is disconnected, and repair means a disconnected line is recovered. Now performance metrics such as number of damaged branches and the mean recovery time can be derived from the Markov transition diagram in Figure 2. Let L be the expected damaged branches, and L_q be the damaged branches waiting for being repaired. Then

$$L = \sum_{k=0}^{K} k \pi_k , \qquad (24)$$

$$L_{q} = \sum_{k=0}^{K} (k - R)\pi_{k} , \qquad (25)$$

where π_k is the steady-state probability that the number of damaged branches is k for for k=0, 1, ..., K. with

$$\pi_{0} = \frac{1}{1 + \sum_{k=0}^{K} c_{k}}, \text{ for } k=0,$$
 (26)

$$\pi_k = c_k \pi_0$$
, for $k=1, 2, ..., K$. (27)

and

$$c_k = {K \choose k} \left(\frac{\lambda}{\mu}\right)^k$$
, for $k=1, 2,, R$, (28)

$$c_k = {K \choose k} \left(\frac{\lambda}{\mu}\right)^k \frac{k!}{R! R^{k-R}}, \text{ for } k=R+1, R+2, \dots, K.$$
 (29)

We are also interested in the duration of recovering a damaged branch. Let W be the duration from when the branch is damaged to when it is recovered. According to the Little's Law, W can be estimated by

$$W = \frac{L}{\sum_{k=0}^{K} (K - k) \lambda \pi_k},$$
(30)

where L is given in Equation (24).

VI. PLANNING FOR SURVIVABILITY

A. System Cost

The goal of the DG planner is to determine the siting and sizing of WT and PV units in the distribution network such that the annualized system cost is minimized. Since the output of WT and PV is stochastic, we minimize the expected annualized cost of the active distribution system. That is

$$C_{DG}(\mathbf{x}) = \phi(r,h) \sum_{i=1}^{m} \sum_{j=1}^{n} \sum_{t=1}^{T} x_{ijt} a_i P_{ijt}^c + t_a \sum_{i=1}^{m} \sum_{j=1}^{n} \sum_{t=1}^{T} z_{ijt} (b_i + c_i) E[P_{ijt}], \quad (31)$$

with
$$\phi(r,h) = \frac{r(1+r)^h}{(1+r)^h - 1}$$
. (32)

In the objective function, $\phi(r,h)$ is the capitla recovery factor used to distribute the capital cost over h year at interest rate r in year t. The value of x_{ijt} is a binary decision variable representing whether DER type i is installed at node j in year t for t=1, 2, ..., T. Here $z_{ijt} = \sum_{k=1}^{t} x_{ijt}$ is the cumulative installation of DER type i on node j by t. Also a_i represents the capacity cost in \$/MW. The capacity of DER type i at node j is represented by P_{ijt}^c . The value b_i represents the operating cost in \$/MWh, and c_i is the cost in \$/MWh of the environmental penalty for conventional energy source from the substation. For renewable energy, c_i is a negative value capturing the government credits or tax rebate. In addition, m is the number of available DER types, n is the number nodes to place DER units, and T is the number of the planning years.

B. Optimization Model

The goal of the model is to determine the generator capacity and placement such that the total system cost in equation (31) is minimized while the LOLP and power quality are assured. Such a design can be translated into the following optimization model,

Problem P1

Minimize:
$$f(\mathbf{x}) = C_{DG}(\mathbf{x})$$
 (33)

Subject to:

$$\mu_{P(\mathbf{x})} \ge \mu_D + Z_{1-\alpha} (\sigma_{P(\mathbf{x})}^2 + \sigma_D^2)^{1/2}, \text{ for } \forall t$$
 (34)

$$V_{\min} - Z_{(1-\alpha_2)/2} \sigma_{V_{ji}(\mathbf{x})} \le \mu_{V_{ji}(\mathbf{x})} \le V_{\max} + Z_{(1-\alpha_2)/2} \sigma_{V_{ji}(\mathbf{x})}, \text{ for } \forall j \text{ and } \forall t. \quad (35)$$

$$\sum_{i=1}^{m} x_{ijt} \le 1, \text{ for } \forall j \text{ and } \forall t$$
 (36)

$$z_{iji} = \sum_{i} x_{ijk}$$
 for $\forall i, \forall j$ and $\forall t$ (37)

$$x_{ijt} \in \{0, 1\}, \text{ for } \forall i, \forall j, \text{ and } \forall t$$
 (38)

The objective function (33) is to minimize the annualized system cost. The LOLP is defined by constraint (34). The power quality is governed by constraint (35), and its detailed derivation is available in [22]. Note that $\mu_{\nu_{\mu}(x)}$ is the mean voltage at node j in year t, and $\sigma_{\nu_{\mu}(x)}$ is the voltage standard deviation at node j in year t. Constraint (36) simply states that no more than one DER unit is placed on a node in year t. This condition however can be relaxed if there is no space limitation on the placement of DER units.

Problem P1 belongs to the class of mixed-integer, nonlinear programming problems. This type of problem in general is difficult to solve due to the combinatorial nature combined with the non-linearity issue. For instance, given a 9-node network with five types of DER units, the number of decision variables reaches 135 for a three-year planning. For a ten-year planning, the total decision variables become 450. As the number of decision variables increases, more advanced solution techniques are required. In the next section, we decompose a 9-node three-year DG planning problem into a three-phase optimization model, each being solved sequentially using Microsoft Excel with the Solver Add-in, and the results are further verified by commercial solver Cplex.

VII. NUMERICAL EXPERIMENT

A. Network Topology and Load Profile

In this section, we solve a simple network to demonstrate the application and performance of Problem P1. Originally from [23], the network in Figure 3 consists of nine nodes that distribute power to end consumers through eight branches. Node 9 is intended for a location of the substation because substation handles large buck energy, and it shall be placed in the center of the network. Nodes 1 through 8 are the locations where wind turbines and PV panels can be paced during the planning horizon. There are seven types of DER units available: three wind turbines (1 MW, 2 MW, and 3 MW); two PV systems (0.25 MW and 0.5 MW); and two substations (45 MW and 50 MW). Here substations are treated as DER units just for mathematical convenience. Without loss of generality, line resistance between two adjacent nodes is assumed to be 1 Ω . We adopt the DC circuit to demonstrate the proposed DG integration by considering the fact that the system is planned at the strategic level with less influence of reactive power.

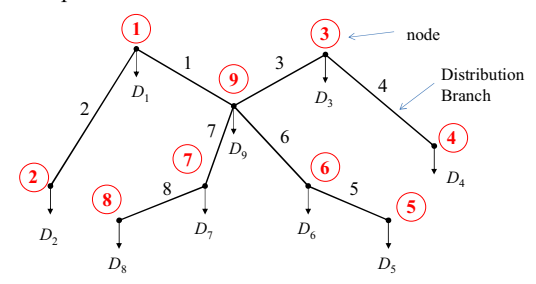


Figure 3: A 9-Node Distribution Network [23]

Table 1 lists the demand growth over the 3-year period. In this study, it is assumed that both the mean and the variance increase with the time. The LOLP criterion is set with α_1 =0.01 and the power quality confidence is α_2 =0.9. The nominal voltage is $V_{\rm DG}$ =33 KV, and the upper and lower voltage is $V_{\rm max}$ =1.95 $V_{\rm DG}$ and $V_{\rm min}$ =1.95 $V_{\rm DG}$, respectively.

Table 1: Mean and Variance of Load in Three Years (Unit: MW)

	ח	Ye	ear 1	Ye	ar 2	Year 3		
j	D_j	$E[D_j]$	$Var(D_i)$	$E[D_j]$	$Var(D_i)$	$E[D_j]$	$Var(D_j)$	
1	D_1	7.640	0.146	7.869	0.155	8.105	0.164	
2	D_2	8.720	0.190	8.982	0.201	9.251	0.213	
3	D_3	4.580	0.052	4.717	0.055	4.859	0.058	
4	D_4	4.000	0.040	4.120	0.042	4.244	0.045	
5	D_5	5.140	0.066	5.294	0.070	5.453	0.074	
6	D_6	6.110	0.093	6.293	0.099	6.482	0.104	
7	D_7	7.640	0.146	7.869	0.155	8.105	0.164	
8	D_8	7.270	0.132	7.488	0.140	7.713	0.148	
9	D_9	0.000	0.000	0.000	0.000	0.000	0.000	
System		51.10	0.865	52.63	0.917	54.21	0.972	

Table 2 presents the costs associated with equipment installation, maintenance and carbon credits. Capacity factor computes the mean output power of a DER unit relative to its name-plated capacity. Though the values of capacity factor vary with the local wind speed and solar radiation, it has less impact on the justification of the survivability of the distribution power via defensive microgrid operation.

Table 2: Power Capacity and Costs for DER Units (SS=Substation)

i	DER	$P_i^{(c)}$	a_i	b_i	c_i	Capacity
	Type	(MW)	(\$/MW)	(\$/MWh)	(\$/MWh)	factor
1	WT1	1	910,000	10	-5	0.4
2	WT2	2	773,500	9	-5	0.35
3	WT3	3	637,000	8	-5	0.3
4	PV1	0.25	2,000,000	3	-10	0.3
5	PV2	0.5	1,750,000	2	-10	0.3
6	SS1	45	273,000	16	10	1.0
7	SS2	50	227,500	16	10	1.0

B. The Result of Siting and Sizing

Based on the data in Tables 1 and 2, we use Excel solver to find the sizing and sizing of DER for three years, and the results are summarized in Table 3. For year 1, nodes 2, 4, and 6 the equipment chosen were 2 MW wind turbines. For nodes 1 and 8 the equipment chosen were 3 MW wind turbines. As for node 9, it is only intended for a substation. The optimal solution chosen was SS2 that produces 50MW. For year 2, the equipment chosen for nodes 2 and 7 were 3 MW wind turbines. Finally in year 3, the optimal solution of equipment added to nodes 4 through 7 were PV panels with 0.5 MW. For node 8 the equipment chosen were 3 MW wind turbines. The optimal solution resulted in a total cost of \$13,706,237 for total three years.

	DER\Node	1	2	3	4	5	6	7	8	9
	WT1									
r I	WT2		1		1		1			
Year 1	WT3	1							1	
	PV1									
	PV2									
	SS1									
	SS2									1
	DER\Node	1	2	3	4	5	6	7	8	9
	WT1									
.,	WT2									
rear 2	WT3		1					1		
Ď	PV1									
	PV2									
	SS1									
	SS2									
	DER\Node	1	2	3	4	5	6	7	8	9
	WT1				<u> </u>			<u> </u>	Ü	_
	WT2									
0	WT3							_	1	
Year 3	PV1									
	PV2				1	1	1	1		
	SS1									
	992									

C. Prevention

The protection for the power supply in the 9-node distribution network is achieved by progressively integrating WT and PV units across nodes 1-8 over the three years. Table 4 summarizes the amount of the power being protected from years 1 to 3 by computing the maximum available power of DER power of individual nodes. For instance, in Year 1, WT3 is installed on node 1, this means 39.3% of 7.64 MW load is protected by the local microgrid because the maximum

capacity of WT3 is 3 MW. In year 3, note 8 have installed total 6 MW microgrid power, thus 6/7.713=77.8% of the local demand is protected. At the system level, the annual protected power is 23.6% in year one, 34.2% in year two and 42.4% in year three. This simple example clearly shows that distributed power integration can effectively prevent or protect the power shortage in contingency when the substation or the distribution lines are damaged.

Table 4: The Amount of Power Being Protected in Years 1-3

				Year 1					
Node j	1	2	3	4	5	6	7	8	9
Mean (MW)	7.640	8.720	4.580	4.000	5.140	6.110	7.640	7.270	0
Microgrid (MW)	3	2	0	2	0	2	0	3	0
Protection (%)	39.3	22.9	0.0	50.0	0.0	32.7	0.0	41.3	0
				Year 2					
Node j	1	2	3	4	5	6	7	8	9
Mean (MW)	7.869	8.982	4.717	4.120	5.294	6.293	7.869	7.488	0
Microgrid (MW)	3	5	0	2	0	2	3	3	0
Protection (%)	38.1	55.7	0.0	48.5	0.0	31.8	38.1	40.1	0
				Year 3					
Node j	1	2	3	4	5	6	7	8	9
Mean (MW)	8.105	9.251	4.859	4.244	5.453	6.482	8.105	7.713	0
Microgrid (MW)	3	5	0	2.5	0.5	2.5	3.5	6	0
Protection (%)	37.0	54.0	0.0	58.9	9.2	38.6	43.2	77.8	0

D. Survivability

A key criterion to measure the survivability is to assess the robustness of the distribution when it is attacked by extreme weather events or other natural disasters. Let us consider one extreme case where the substation power is totally lost while all the distribution branches are still connected and functional. Since it is in the contingent mode, we also assume the power demand of each node is reduced by 50 percent to maintain the operation of critical loads. We compute the survivability for years 1 to 3 and the results are summarized in table 5. As shown in the table, node 4 has the largest survivability with 97.1% of the critical load being met. Moving into year 2, node 2 has the largest survivability with 111.3% of the critical load being met. This implies that node 2 has surplus power that will flow to node 1. Thus the actual power of node 1 increase from 3 MW to 3.51 MW (i.e. 5+3-4.491). In year 3, there are three nodes have surplus power, these are nodes 2, 4, and 8. Obviously the surplus power will enter nodes 1, 3 and 7, respectively. This indeed increases the survivability of the neighborhood nodes.

Table 5: Survivability in Years 1-3 with Lost Substation

				Year 1					
Node j	1	2	3	4	5	6	7	8	9
Mean (MW)	3.935	4.491	2.359	2.060	2.647	3.147	3.935	3.744	0.000
Microgrid (MW)	3	2	0	2	0	2	0	3	0
Survivability (%)	76.2	44.5	0.0	97.1	0.0	63.6	0.0	80.1	0
				Year 2					
Node j	1	2	3	4	5	6	7	8	9
Mean (MW)	3.935	4.491	2.359	2.060	2.647	3.147	3.935	3.744	0.000
Microgrid (MW)	3	5	0	2	0	2	3	3	0
Survivability (%)	76.2	111.3	0.0	97.1	0.0	63.6	76.2	80.1	0
				Year 3					
Node j	1	2	3	4	5	6	7	8	9
Mean (MW)	4.053	4.626	2.429	2.122	2.727	3.241	4.053	3.856	0
Microgrid (MW)	3	5	0	2.5	0.5	2.5	3.5	6	0
Survivability (%)	74.0	108.1	0.0	117.8	18.3	77.1	86.4	155.6	0

E. Recovery

As discussed in Section V, the recovery and repair process depends on the failure rate of the distribution lines and the repair capacity. We compare the recovery time under different weather severity manifested by λ =1line/hour and λ =0.5 line/hour. Obviously higher value of λ implies a harsher weather condition. K=8 because there is eight distribution branches in Figure 3, and K=2 means two teams are available performing the recovery job. We compute the expected number of failed lines K and the expected recovery time K per line based on Equations (24) and (30), respectively. Both K and K are calculated as the repair rate K increases from 0.1 to 5 line/hour. Usually the repair rate is proportional to the size of the repair team. The results are shown in Figures 4 and 5.

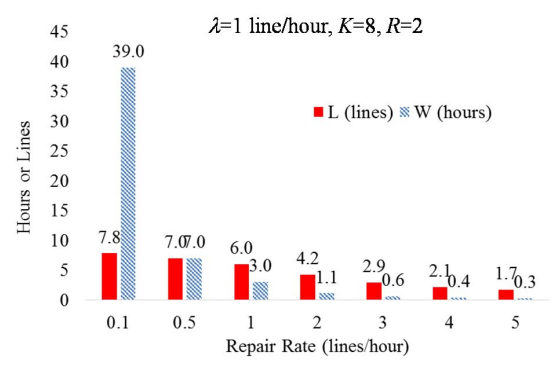


Figure 4: Recovery Time and Disconnected Branches with $\lambda=1$, R=2

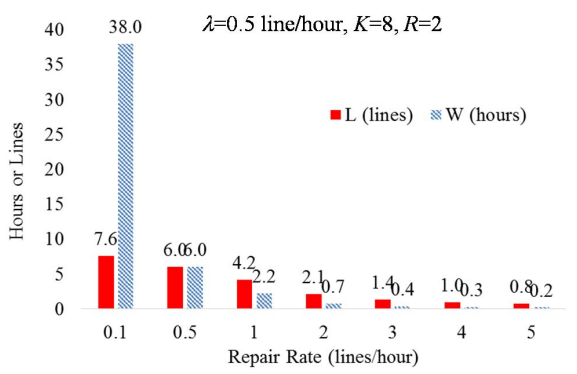


Figure 5: Recovery Time and Disconnected Branches with λ =0.5, R=2

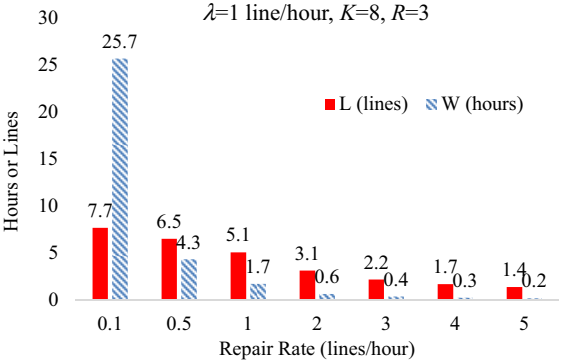


Figure 6: Recovery Time and Disconnected Branches with $\lambda=1$, R=3

There are two observations made from Figures 4 and 5. First, μ has a decisive role in terms of the recovery time. For instance, with μ =0.1 line/hour, it takes 39 hours for bringing a damaged branch back to operation under a severe weather. However, even if the weather severity is reduced by a half (from λ =1 to λ =0.5), the duration of the recovery is still 38 hours per line under μ =0.1 line/hour. Finally we examine whether increasing the number of repair teams can expedite the recovery time. In Figure 6, we increases R to 3, and recompute L and W under λ =1. The recovery time is reduced from 39 hours to 25.7 hours, but the effectiveness is not very impressive compared with the result if increasing the repair rate to 0.5 lines/hour. The latter is able to restore a line within 4.3 hours.

VIII. CONCLUSION

This paper presents a probabilistic framework to plan and analyze the resilience of distribution grid via variable power integration. We approach the grid resilience from three aspects: prevention, survivability, and recovery. Prevention is achieved through pro-active maintenance by inspecting and replacing aging components prior to failure. Prevention can also be realized through the integration of variable microgrid power for increasing the supply robustness. Survivability is attained through the defensive microgrid operation and topological reconfiguration in contingency. Recovery is assessed and planned through the machine-repairman Markov model. The variations of power, load and voltage are captured by the first and second moments and the chance constraints.

Three observations are obtained from the numerical example. First, the 9-node testing network indicates that 100 percent of power protection can be achieved sequentially in three years by concurrently injecting WT and PV units. Second, the most influential factor affecting the recovery time is the repair rate, not necessary the weather severity and the number of repair teams. Third, wind- and solar-based microgrid generation is advantageous over fuel-based generator against cascading failures. This is because the lifetime of fuel supply is likely to be destroyed post the attack of extreme weather or earthquake. Since WT and PV generation relies on the natural resources, there is no need of fuel supply. For the future effort, we will incorporate the occurrence rate and the duration of extreme events in the planning model that will be tested in a setting of large and complex grid systems.

ACKNOWLEDGMENT

This project is partially funded by NSF (grant #: 1704933) and Texas State University REP (grant #: 2000021000).

REFERENCES

[1] L. Carlson, G. Bassett, M. Buehring, M. Collins, S. Folga, B. Haffenden, F. Petit, J. Phillips, D. Verner, R. Whitefield, Resilience: Theory and Applications. Argonne National Laboratory Report, pp. 1-64, 2012, available at http://www.ipd.anl.gov/anlpubs/2012/02/72218.pdf, (accessed on Nov. 2, 2017).

- [2] M. Panteli, P. Mancarella, "The grid: Stronger, bigger, smarter?: Presenting a conceptual framework of power system resilience," IEEE Power Energy Magazine, vol. 13, no. 3, 2015, pp. 58-66.
- [3] U.S. Department of Commerce (US DoC), Economic Impact of Hurricane Sandy, Report prepared by Economics and Statistics Administration Office of the Chief Economist, 2013, available at http://www.esa.gov/sites/default/files/sandyfinal101713.pdf (accessed on Dec. 25, 2016).
- [4] B. Zhou, L. Gu, Y. Ding, L. Shao, et al., "The great 2008 Chinese ice storm: Its socioeconomic-ecological impact and sustainability lessons learned," Bulletin of the American Meteorological Society, vol. 92, no. 1, 2014, pp. 47-60.
- [5] Y. Lin, Z. Bie, "Study on the resilience of the integrated energy system," Energy Procedia, vol. 103, December, 2016, pp. 171-176.
- [6] B. Ovens, "The rise of distributed power," Report of General Electric, 2014, http://www.eenews.net/assets/2014/02/25/document_gw_02.pdf, (last accessed on Nov. 10, 2017).
- [7] B. Li, R. Roche, A. Miraoui, "A temporal-spatial natural disaster model for power system resilience improvement using DG and lines hardening," in Proceedings of 2017 IEEE Manchester PowerTech, 2017, pp. 1-6.
- [8] Y. Wang, C. Chen, J. Wang, R. Baldick, "Research on resilience of power systems under natural disasters—A review," IEEE Transactions on Power Systems, vol. 31, no. 2, 2016, pp. 1604-1613.
- [9] A. Kwasinski, V. Krishnamurthy, J. Song, R. Sharma, "Availability evaluation of micro-grids for resistant power supply during natural disasters," IEEE Transactions on Smart Grid, vol. 3, no. 4, 2012, pp. 2007-2018.
- [10] M. Panteli, D.N. Trakas, P. Mancarella, N.D. Hatziargyriou, "Boosting the power grid resilience to extreme weather events using defensive islanding," IEEE Transactions on Smart Grid, vol. 7, no. 6, 2016, pp. 2913-2922.
- [11] C. Shao, Y. Ding, J. Wang, Y. Song, "Modeling and integration of flexible demand in heat and electricity integrated energy system, IEEE Transactions on Sustainable Energy, vol. 9, no. 1, 2018, pp. 361-370.
- [12] Z. Bie, Y. Lin, G. Li, F. Li, "Battling the extreme: a study on the power system resilience," in Proceedings of the IEEE, vol. 105, no. 7, 2017, pp. 1253-1265.
- [13] X. Liu, M. Shahidehpour, Z. Li, X. Liu, Y. Cao, Z. Bie, "Microgrids for enhancing the power grid resilience in extreme conditions," IEEE Transactions on Smart Grid, vol. 8, no. 2, 2017, pp. 589-597.
- [14] EPRI, Grid Resiliency, 2017, available https://www.epri.com/#/pages/sa/grid_resiliency (accessed on Nov. 11, 2017).
- [15] ERCOT, "ERCOT responds to Hurricane Harvey," Sept. 6, 2017, available http://www.ercot.com/help/harvey (accessed on Dec. 4, 2017).
- [16] C. Novoa, T. Jin, "Reliability centered planning for distributed generation considering wind power volatilities," Electronic Power Systems Research, vol. 81, no. 8, 2011, pp. 1654-1661.
- [17] M. Lave, J. Kleissl, "Optimum fixed orientations and benefits of tracking for capturing solar radiation," Renewable Energy, vol. 36, no. 3, 2011, page 1145-1152.
- [18] Z.M. Salameh, B.S. Borowy, A.R.A Amin, "Photovoltaic module-site matching based on the capacity factors," IEEE Transactions on Energy Conversion, vol. 10, no. 2, 1995, pp. 326-332.
- [19] O. Tor, M. Shahidehpour, "Power distribution asset management," in Proceedings of IEEE Power Engineering Society General Meeting, 2006, pp.1-7.
- [20] T. Jin, Y. Tian, C.W. Zhang, D. Coit, "A multi-criteria planning for distributed wind generation under strategic maintenance," IEEE Transactions on Power Delivery, vol. 28, no. 1, 2013, pp. 357-367.
- [21] E. Elsayed, Reliability Engineering, Chapter 8, 2nd Edition, 2012, Wiley & Sons, Hoboken, NJ, USA.
- [22] T. Jin, Y. Yu, E. Elsayed, "Reliability and quality control for distributed wind-solar energy integration: A multi-criteria approach," IIE Transactions, vol. 47, no. 10, 2015, pp. 1122-1138.
- [23] W. El-Khattam, K. Bhattacharya, Y. Hegazy, M. Salama, "Optimal investment planning for distributed generation in a competitive electricity market," IEEE Transactions on Power Systems, vol. 19, no. 3, 2004, pp. 1674-1684.